

# *Thermoresponsive engineered emulsions stabilised with branched copolymer surfactants for nasal drug delivery of molecular therapeutics*

Article

Published Version

Creative Commons: Attribution 4.0 (CC-BY)

Open Access

Rajbanshi, A., Hilton, E., Atkinson, E., Phillips, J. B., Vanukuru, S., Khutoryanskiy, V. V. ORCID: <https://orcid.org/0000-0002-7221-2630>, Gibbons, A., Falloon, S., Dreiss, C. A., Murnane, D. and Cook, M. T. (2025) Thermoresponsive engineered emulsions stabilised with branched copolymer surfactants for nasal drug delivery of molecular therapeutics. *International Journal of Pharmaceutics*, 676. 125506. ISSN 0378-5173 doi: 10.1016/j.ijpharm.2025.125506 Available at <https://centaur.reading.ac.uk/122307/>

It is advisable to refer to the publisher's version if you intend to cite from the work. See [Guidance on citing](#).

To link to this article DOI: <http://dx.doi.org/10.1016/j.ijpharm.2025.125506>

Publisher: Elsevier

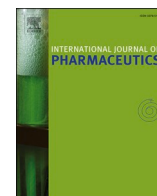
All outputs in CentAUR are protected by Intellectual Property Rights law, including copyright law. Copyright and IPR is retained by the creators or other copyright holders. Terms and conditions for use of this material are defined in the [End User Agreement](#).

[www.reading.ac.uk/centaur](http://www.reading.ac.uk/centaur)

## **CentAUR**

Central Archive at the University of Reading

Reading's research outputs online



# Thermoresponsive engineered emulsions stabilised with branched copolymer surfactants for nasal drug delivery of molecular therapeutics

Abhishek Rajbanshi<sup>a,b,\*</sup>, Eleanor Hilton<sup>b</sup>, Emily Atkinson<sup>b</sup>, James B. Phillips<sup>b</sup>, Shiva Vanukuru<sup>a,c</sup>, Vitaliy V. Khutoryanskiy<sup>c</sup>, Adam Gibbons<sup>d</sup>, Sabrina Falloon<sup>d</sup>, Cecile A. Dreiss<sup>e</sup>, Darragh Murnane<sup>a</sup>, Michael T. Cook<sup>b</sup>

<sup>a</sup> School of Life and Medical Science, University of Hertfordshire, Hatfield, Hertfordshire AL10 9AB, UK

<sup>b</sup> UCL School of Pharmacy, University College London, 29-39 Brunswick Square, London WC1N 1AX, UK

<sup>c</sup> School of Pharmacy, University of Reading, Reading, Berkshire RG6 6UR, UK

<sup>d</sup> Bepak, Bergen Way, King's Lynn, Norfolk PE30 2JJ, UK

<sup>e</sup> Institute of Pharmaceutical Science, King's College London, London SE1 8WA, UK

## ABSTRACT

Novel branched copolymer surfactants (BCS) allow the formation of oil-in-water emulsions that exhibit a temperature-induced liquid-to-gel transition. If the temperature of this transition is between room and body temperature (ca 25 and 37 °C, respectively), then the emulsions form a gel *in situ* upon contact with the body. A major advantage of this *in situ* gelation is the potential to manipulate the materials at room temperature in the low viscosity liquid state, then administer them to the body to initiate a switch to a retentive gel state, which could be used to deliver drugs to challenging sites such as the nasal mucosa. There are, however, several important factors which have not been explored for thermoresponsive BCS-stabilised emulsions to progress their use towards this application. Neither the delivery of drugs from the materials, the retention on tissue, nor the impact of co-formulated drugs on the thermoresponsive behaviours, are known. Furthermore, it has not been demonstrated that the materials are compatible with devices to generate sprays of the correct profiles for nasal administration. In this study we investigate the potential of thermoresponsive BCS-stabilised emulsions for the nasal delivery of licensed molecular therapeutics to examine the potential of BCS emulsion systems as a carrier for medicines. It was found that thermoresponsive behaviours can be maintained in the presence of drug substances, and that the liberation of the incorporated drugs occurs in a sustained manner. The BCS appear to have comparable cytotoxicity to common excipients and significantly enhanced retention on nasal tissue compared to even well-established mucoadhesives. The emulsions were incorporated into a spray device to demonstrate that the materials can be atomised with a plume appropriate for nasal administration prior to *in situ* gelation.

## 1. Introduction

Intranasal drug delivery is a route of administration that can enable therapies which would be ineffective or inefficient via other means. The nasal cavity contains a large and highly vascularised surface area, allowing for efficient drug absorption while bypassing first-pass metabolism (Bhise et al., 2008; Ong et al., 2016; Pozzoli et al., 2016). Common uses include local administration of drugs for treating conditions such as nasal congestion, infections, and allergic rhinitis (Illum, 2003). Additionally, nasal delivery can also be employed for the systemic delivery of drugs to treat diseases like osteoporosis, migraine, pain, and for vaccine administration (Rama Prasad, Krishnaiah and Satyanarayana, 1996). This method offers rapid drug onset, high patient compliance, and can bypass the blood–brain barrier via the olfactory bulb (Costantino et al., 2007; Lee and Minko, 2021). For

neurotherapeutic agents intranasal delivery ensures rapid onset of drug action, improved bioavailability, reduced dosage, and fewer side effects (Bahadur and Pathak, 2012; Kapoor, Cloyd and Siegel, 2016; Rassu et al., 2017). Various dosage forms are available for nasal drug delivery, suspension nasal sprays and nasal drops being the most popular (Ehrick et al., 2013). Aqueous nasal spray formulations are favoured for their simplicity, drug compatibility, rapid onset and ease of administration (Ehrick et al., 2013; Pires et al., 2022). Despite this, they face challenges such as short residence time and limited drug retention due to mucociliary clearance and gravity (Ehrick et al., 2013; Saindane, Pagar and Vavia, 2013). Enhancing residence time on the nasal mucosa can be achieved through the use of mucoadhesive and/or viscous materials (Leung and Robinson, 1987). For example, highly-viscous polymers solutions, such as carbomers or xanthan gum, have been shown to adhere to the nasal mucosa for long periods, allowing for prolonged and

\* Corresponding author at: School of Life and Medical Sciences, University of Hertfordshire, Hatfield, Hertfordshire AL10 9AB, UK.

E-mail address: [a.rajbanshi@herts.ac.uk](mailto:a.rajbanshi@herts.ac.uk) (A. Rajbanshi).

<https://doi.org/10.1016/j.ijpharm.2025.125506>

Received 26 January 2025; Received in revised form 20 March 2025; Accepted 21 March 2025

Available online 5 April 2025

0378-5173/© 2025 The Author(s). Published by Elsevier B.V. This is an open access article under the CC BY license (<http://creativecommons.org/licenses/by/4.0/>).

controlled drug release (Vigani et al., 2020). However, there are drawbacks associated with viscous polymeric solutions as a nasal spray formulation; typically they cannot be actuated through nozzles or atomised into a fine mist, resulting in inconsistent and inefficient dosing (Moakes et al., 2021).

“Engineered” emulsions stabilised by copolymer surfactants that respond to temperature stimuli to induce a sol–gel transition offer great potential for nasal drug delivery (da Silva et al., 2022; Rajbanshi et al., 2022). Previous studies have identified branched copolymer surfactants (BCSs) as optimal for in-situ gelation due to their superior stability, provided by steric hindrance and multipoint irreversible anchoring at the oil–water interface compared to linear copolymers (Rajbanshi et al., 2024). The latter sol–gel transition could provide a novel approach for nasal mucoadhesion, thereby optimizing nasal drug delivery. Not only this, but BCSs can also be synthesised with relative ease in a highly scalable one-pot synthesis (Rajbanshi et al., 2024).

Herein, we evaluated a BCS consisting of thermoresponsive diethylene glycol methyl ether methacrylate (DEGMA), hydrophilic polyethylene glycol monomethacrylate (PEGMA), branching ethylene glycol dimethacrylate (EGDMA), and hydrophobic dodecanethiol (DDT). This BCS, identified in our previous work, forms a viscous gel state at nasal cavity temperatures (32–35 °C) (Rajbanshi et al., 2023a, b). Emulsions stabilised by this BCS alone, and in combination with methylcellulose, were tested for their ability to solubilise various active pharmaceutical ingredients (APIs), control release kinetics, and provide compatibility with nasal devices. The APIs investigated were phenylephrine hydrochloride, lidocaine hydrochloride, and budesonide, chosen for their varying solubility and partition coefficients. Rheological analysis and spray performance testing were performed to assess the suitability of drug-loaded emulsions for nasal administration.

## 2. Experimental

### 2.1. Materials and methods

Di(ethylene glycol) methyl ether methacrylate (DEGMA, 95 %), poly(ethylene glycol) methyl ether methacrylate (PEGMA,  $M_n$  950  $\text{gmol}^{-1}$ ), ethylene glycol dimethacrylate (EGDMA, 98 %), 1-dodecanethiol (DDT, 99 %), anhydrous dodecane (99 %), absolute ethanol, acetonitrile (gradient grade) and methyl cellulose (2000 cP, 2 % aqueous solution at 20 °C) were purchased from Sigma-Aldrich (UK).  $\alpha,\alpha$ -azobisisobutyronitrile (AIBN, >99 %) was obtained from Molekula (UK). Sodium dihydrogen phosphate dihydrate (99 %), orthophosphoric acid (85 %), potassium dihydrogen phosphate (99 %) and 1-octanesulphonic acid sodium salt (98 %) were supplied by VWR (UK). Dialysis tubing with molecular weight cut off (MWCO) of 14 kDa was purchased from Sigma Aldrich (UK). Chitosan (50–190 kDa; deacetylation degree  $20.8 \pm 0.5$  %), dextran (average molecular weight 4000 Da), phenylephrine hydrochloride and lidocaine hydrochloride were purchased from Sigma Aldrich (UK). Micronised budesonide was supplied by LMG Pharma (Boca Raton, USA). Phosphate buffered saline (PBS) tablets were purchased from Oxoid (UK). Tween 20 was purchased from Fluka Analytical, UK. Potassium dihydrogen orthophosphate, octane sulphonic acid sodium salt, orthophosphoric acid, sodium dihydrogen phosphate dihydrate, absolute ethanol, and gradient grade acetonitrile were purchased from VWR (UK). Deionised water was employed in all experiments and produced in-house by reverse osmosis. All chemicals were used as received. Mechanical nasal spray pumps delivering 100  $\mu\text{L}$  of formulation per actuation were provided by Bepak. The optimal BCS system was synthesised and described in our previous studies (denoted as BSC5) (Rajbanshi et al., 2023a; Rajbanshi et al., 2023b).

### 2.2. Emulsion formation with drug loading

Aqueous BCS solutions (20 wt%) were prepared in cold water. If required, 0.25 wt% methylcellulose (MC) additive was added in a

second mixing step. For emulsion formulations with APIs incorporated, 0.5 wt% phenylephrine HCl, 5 wt% lidocaine HCl and 0.064 wt% budesonide (as a suspension) were then added to the aqueous solution to match licensed reference products (Martindale Pharma an Ethypharm Group Company, 2017; Sandoz Limited, 2022). The mixtures were refrigerated and mixed by vortex every 15 min until a clear solution was obtained for lidocaine and phenylephrine. Budesonide solution was fully saturated in the BCS aqueous phase, leaving excess solid. Dodecane was added and the system emulsified as described above to yield a three phase system of undissolved drug, aqueous phase, and creamed emulsion phase. This saturated emulsion phase was then isolated for future experiments, including the determination of loading efficiency.

The preparation of oil-in-water emulsions was carried out by mixing an equal amount of aqueous BCS solution with an equal amount of dodecane oil in a 1:1 ratio. For details of the specific composition of emulsion formulation, see Table 1. The mixtures were emulsified for 2 min using a Silverson L4R mixer with a 5/8" micro tubular frame and integral general purpose disintegrating head at 2400 rpm. Upon emulsification, the mixtures were left to rest for 36 h at room temperature. The resulting creamed phases of the emulsions were then isolated by removal of the upper turbid phase for further analysis. For details on emulsion mass yields see the [supplementary information](#).

### 2.3. Rheology of thermoresponsive emulsions

Rheology experiments were performed on an AR 1500ex rheometer (TA instruments (USA)) equipped with a Peltier temperature control unit and a 40 mm parallel plate geometry with a specified gap distance of 500–750  $\mu\text{m}$ . The creamed layer of each emulsion (collected after 36 h of isolation) was placed on the rheometer lower plate prior to the measurement. Samples were equilibrated for 2 min prior to the measurements. Temperature ramps were performed in the range 20–50 °C, at 1 °C  $\text{min}^{-1}$  heating rate, with an oscillating stress of 1 Pa and a frequency of 6.283 rad/s. The change in storage modulus ( $G'$ ) and loss modulus ( $G''$ ) as a function of temperature were recorded.

### 2.4. Droplet size determination of emulsion by laser diffraction

Emulsion droplet size (36 h after isolation of the creamed phase) was determined by laser diffraction using Sympatec HELOS/BR QUIXEL. 10  $\mu\text{L}$  of emulsion was added to the dispenser R3 cuvette containing 50 mL of water with constant stirring at 1800 rpm. Water was used as a reference before sample measurement. All samples were measured at an optical concentration of approximately 30 %. Trigger conditions were as follows: reference measurement duration – 10 s, signal integration time – 100 ms, trigger timeout – 90 s.

### 2.5. Chromatographic method for determination of drug concentration

#### 2.5.1. Phenylephrine and lidocaine

Concentrations of phenylephrine and lidocaine released from the emulsion formulations were determined by analytical high performance liquid chromatography (HPLC) using a Waters symmetry C18 column (250 mm x 4.6 mm, 5  $\mu\text{m}$ ). The mobile phase consisted of aqueous phase (0.02 M potassium dihydrogen phosphate, 0.01 M of octane sulphonic acid sodium salt, pH 2.8) and acetonitrile. A gradient method was selected where the gradient began at 0 min 75:25, changed to 70:30 after 10 min, then returned to 75:25 at 21 min (total method 25 min). The flow rate was 1 mL/min at 30 °C, with detection set at 272 nm. A 20  $\mu\text{L}$  injection volume was used for each solution. Method validation adhered to ICH guidelines (Harron, 2013; ICH, 2022). For the evaluation of controlled release, the validation range covered 20 %, 40 %, 60 %, 80 %, 100 % and 120 % of the target concentration in phosphate buffer saline solution (0.05 mg for phenylephrine and 0.5 mg for lidocaine). Precision and repeatability assessments were conducted with six replicates at the target concentrations of phenylephrine (0.05 mg/mL) and



**Table 1**  
Reagent and drug quantities for emulsion formulation.

Reagents	Phenylephrine		Lidocaine		Budesonide	
	Emulsion with BCS	Emulsion with BCS/MC	Emulsion with BCS	Emulsion with BCS/MC	Emulsion with BCS	Emulsion with BCS/MC
BCS	0.5	0.5	0.5	0.5	0.5	0.5
Methylcellulose		0.0125		0.0125		0.0125
Phenylephrine	0.025	0.025				
Lidocaine			0.25	0.25		
Budesonide					0.0032	0.0032
Water	2.24	2.23	2.13	2.12	2.25	2.24
Dodecane oil	2.24	2.23	2.13	2.12	2.25	2.24

lidocaine (0.5 mg/mL). Calibration curves were constructed from accuracy data, plotting peak area versus concentration to verify linearity.

2.5.2. Budesonide

Concentrations of budesonide were quantified using an isocratic HPLC method described with a Waters stainless steel column (150 mm x 4.6, 3 μm, end-capped octadecyl silyl silica gel). The mobile phase consisted of ethanol, acetonitrile, and phosphate buffer solution (PBS) (2:34:66 by volume, 0.026 M sodium dihydrogen phosphate dihydrate, pH 3.2). The flow rate was 1.5 mL/min at 50 °C, with detection set at 240 nm. A 20 μL injection volume was used for each solution. Method validation adhered to ICH guidelines (Harron, 2013; ICH, 2022). Accuracy testing was carried out on 7 concentrations of 0.01 mg/mL, 0.02 mg/mL, 0.04 mg/mL, 0.06 mg/mL, 0.08 mg/mL, 0.1 mg/mL and 0.12 mg/mL of budesonide in 0.2 %v/v Tween-20 in PBS as a solvent. Precision and repeatability were tested with six determinations at the target concentration (0.1 mg/mL). Calibration curves were constructed from accuracy data, plotting peak area versus concentration to verify linearity.

2.6. Drug quantification and release profile using Franz diffusion cells

Quantitative analysis of the emulsion drug loading was performed using the HPLC methods previously described (section 2.3). For phenylephrine and lidocaine, 1 g of creamed emulsion (equivalent to 5 mg of phenylephrine, and 25 mg of lidocaine) was weighed and dissolved in 100 mL of aqueous mobile phase. For quantification of budesonide by HPLC, 1.5 g of emulsion (equivalent to 1 mg of budesonide) was dissolved in 10 mL of the mobile phase. Sample solutions were sonicated for 10 min, then centrifuged for 15 min (5000 rpm). The supernatants were collected for analysis, where drug content was determined using calibration curves. For budesonide, calculations were based on the sum of the areas of the two epimer peaks (see Supplementary Fig. S3).

For release studies, individually calibrated upright unjacketed Franz diffusion cells (Soham Scientific, average volume 3 mL, diameter 1 cm) were used. A dialysis membrane (MWCO 12–14 kDa) was mounted between the donor and receiver chambers of the cells. The receiver

chamber was filled with PBS of pH 7.4 for phenylephrine and lidocaine determination, and with 0.2 %v/v Tween-20 in PBS of pH 7.4 for budesonide determination. 0.5 g of phenylephrine emulsion (equivalent to 2.5 mg phenylephrine), 0.5 g of lidocaine emulsion (equivalent to 25 mg lidocaine) and 0.1 g of budesonide emulsion (equivalent to 32 μg budesonide) was added to the donor chamber of the Franz cell. Sink conditions were maintained as per the solubility of the drugs (Table 2). Franz cells were equilibrated in a water bath at 37 °C for 0.5 h with stirring in the receptor chamber during the diffusion study (to achieve a temperature in the donor chamber temperature of 32 °C, representing the nasal mucosa surface temperature). Samples (100 μL from each of six Franz cell replicates) of the receiver fluid were withdrawn at intervals up to 24 h and replaced with preheated receiver fluid. Drug quantification was achieved using HPLC.

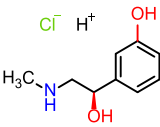
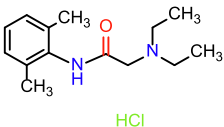
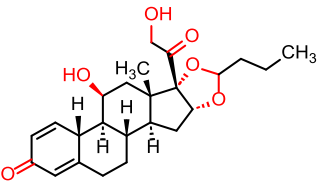
2.7. Mathematical modelling of drug release kinetics and statistical analysis

To study the drug release profile of all 3 APIs studied, Korsmeyer-Peppas model was applied to fit the experimental data. The model is described by the equation

$$M_t/M_\infty = K_m t^n$$

where,  $M_t$  and  $M_\infty$  represent cumulative drug release at time  $t$  and at infinite time, respectively.  $K_m$  is a constant related to the structural and geometrical characteristic of the particles,  $t$  is the release time, and  $n$  is the diffusional exponent indicating the drug release mechanism. For thin film delivery systems,  $n = 0.50$  indicates a Fickian diffusion release mechanism,  $0.50 < n < 1.0$  indicates anomalous (non-Fickian) transport and  $n > 1.0$  indicates zero-order release. For budesonide, data were also fitted with linear regression indicating zero order release to assess the best possible release kinetics. The statistical significance of the obtained values was analysed using the Bonferroni post-hoc  $t$ -test for analysis of variance (ANOVA) with GraphPad Prism.

**Table 2**  
Properties of phenylephrine, lidocaine and budesonide (VCCLAB, 2023).

Properties	Phenylephrine	Lidocaine	Budesonide
Structure			
Chemical Formula	C <sub>9</sub> H <sub>14</sub> ClNO <sub>2</sub>	C <sub>14</sub> H <sub>25</sub> ClN <sub>2</sub> O <sub>2</sub>	C <sub>25</sub> H <sub>34</sub> O <sub>6</sub>
Molar mass (g/mol)	167	234	431
Water solubility at 20 °C (mg/mL)	22.0	0.593	0.0457
logP	−0.69	1.81	2.42

## 2.8. Model formulation for nasal device

Dodecane in water (1:1) emulsions stabilised with 10 wt% BCS were used for the investigation of nasal spray generation with a unit dose nasal spray device (NasaDose™) (Recipharm, 2023). The nasal sprays (10 devices for each test) were assembled and parameters such as shot weight, droplet size distribution, plume geometry and spray pattern were tested. These parameters are an essential requirement for in vitro bioequivalence studies, quality control and development of nasal sprays.

### 2.8.1. Determination of shot weights

To determine the shot weights, nasal spray devices were filled with 0.1 g of stabilised emulsion, measured precisely using an analytical balance (A 200 S, Sartorius analytic). The devices were actuated with an automated actuator (SPRAYER-module, Sympatec). After each actuation, the device was reweighed on the same analytical balance to determine the delivered mass.

### 2.8.2. Determination of droplet size distribution (DSD)

The droplet size distribution (DSD) was determined by laser diffraction using a Spraytec instrument (Malvern Panalytical). This technique allows for the measurement of size of droplets and particles in real-time. Both 3 cm and 6 cm distances to the measuring zone were tested. Data were acquired during the fully developed spray phase and droplet sizes were represented by  $D_{10}$ ,  $D_{50}$ , and  $D_{90}$ . These values represent 10 %, 50 % and 90 % of the population below the obtained volume droplet size, respectively. The span, which signified distribution width, was determined using the following equation:

$$(D_{90} - D_{10})/D_{50}$$

The fraction of droplets smaller than 10  $\mu\text{m}$  was also recorded.

### 2.8.3. Determination of plume geometry and spray pattern

For the determination of plume geometry and spray pattern, Proveris Sprayview system was used. The images were corrected for distortion, due to the skewed camera perspective, and plume angle was determined manually using CorelDraw X6 software (Corel).

The characterisation of spray patterns was performed by automated image analysis. The approximate centre of mass (COM) was identified, and the maximum and minimum diameters ( $D_{\text{max}}$  and  $D_{\text{min}}$ ) were drawn through this centre to determine the size of the pattern. The ovality ratio ( $D_{\text{max}}/D_{\text{min}}$ ) was calculated as the control of the shape pattern. The spray pattern was determined based on a single spray. Spray pattern measurements were performed at two distances from the actuator tip (3 and 6 cm) at room temperature.

## 2.9. Cytotoxicity measurements

SH-SY5Y human neuroblastoma cells (European Collection of Authenticated Cell Cultures) were cultured in growth media containing 1:1 Hams F12: Eagle's Minimum Essential medium (EMEM) supplemented with 1 % essential amino acid solution, 15 % foetal bovine serum (FBS), 1 % penicillin/streptomycin (P/S) and 2 mM L-glutamine and maintained in a humidified incubator at 37 °C with 5 %  $\text{CO}_2$  in air. Medium was changed every 2–3 days. When 70–80 % confluency was reached, cells were passaged with trypsin-EDTA, centrifuged at 100 g for 5 min, and re-suspended in medium before seeding into flasks or 96 well plates. Cells were used at passage 10.

Cells were seeded into 96 well plates at a density of 50,000 cells/well in 100  $\mu\text{L}$  growth medium and cultured for 24 h. Medium was aspirated from the wells and replaced with 100  $\mu\text{L}$  of sterile filtered medium containing BCS, sodium lauryl sulfate (SLS), Tween 20 (T20) or Tween 80 (T80) with concentrations starting at 20 mg/mL and decreasing in a 1:3 series dilution. Plates were incubated for 24 h and then an equal volume of the Cell TitreGlo™ reagent was added. The reagent lysed the SH-SY5Y cells and reacted with the ATP to produce a luminescent signal

during a 10 min incubation. The plates were loaded into the SpectraMax® plate reader and set to shake for 60 s before luminescence was measured. Triplicate experimental and technical repeats were performed.

## 2.10. Assessment of mucoadhesion

Artificial nasal fluid (ANF) was prepared according to an established protocol, composed of KCl (7.45 g, 127 mmol), NaCl (1.29 g, 17 mmol), and  $\text{CaCl}_2 \cdot \text{H}_2\text{O}$  (0.23 g, 2.2 mmol) (Porfiryeva et al., 2019). The above ingredients were dissolved in deionised water. The solution was left stirring at room temperature until the compounds fully dissolved, then adjusted to pH 5.80 with 1 M HCl (total volume 1 L). ANF solution was kept at 37 °C throughout the experiments using a water bath.

Sheep heads and nasal tissues were received from P.C. Turner Abattoirs (Farnborough, U.K.) immediately after animal slaughter, packed, transported to the laboratory in cold plastic containers, and used within 24 h of collection. The nasal septum mucosal tissues were carefully extracted from sheep heads with bone-cutting shear scissors and then cut into  $1 \times 1$  cm square pieces with disposable sharp blades.

Experiments to evaluate the mucosal retention of emulsions stabilised with BCS and BCS-MC on ex vivo sheep nasal tissues were conducted using a well-established flow-through method involving fluorescent detection with minor modification. Initially, freshly excised nasal tissue was mounted on a microscope glass slide with the mucosal side facing upward, then placed on a substrate fixed at an angle of 20° and pre-rinsed with 1 mL of ANF solution for 1 min to activate the mucins, before commencing each ex vivo mucoadhesion test.

Fluorescence images were captured for the mucosal surface of the nasal tissues using a Leica MZ10F stereomicroscope (Leica Microsystems, U.K.) equipped with a Leica DFC3000G digital camera fitted with a green fluorescence protein (GFP) filter (blue,  $\lambda_{\text{emission}} = 527$  nm) at  $2.5 \times$  magnification, with an exposure time of 160 ms and a  $1.0 \times$  gain. Initially, images of blank nasal tissues were acquired to determine the background fluorescence intensity for each sample before administration of the test material.

ANF solution (pH 5.80) was dripped onto the nasal mucosa at a flow rate of 0.5 mL per min using a syringe pump (total washing time was 60 min). The flow rate mentioned was intentionally set higher than the physiological production rate of nasal fluid for practical reasons. This adjustment was made to expedite the experiments and ensure they could be conducted within a reasonable time frame. The fluorescence microscopy images of the nasal mucosal surface of each sample were acquired at predetermined time points (every 10 min) and then analysed with ImageJ software (NIH, U.S.A.) by measuring the pixel intensity after each wash with ANF. The pixel intensity of the bare samples (nasal mucosa without fluorescent test material) was subtracted from each measurement and data were converted into normalised intensity values using the following equation:

$$\text{Fluorescence Intensity} = \frac{I - I_b}{I_0 - I_b} \times 100\%$$

where  $I_b$  is the background fluorescence intensity of a given tissue sample (a blank tissue);  $I_0$  denotes the initial fluorescence intensity of that sample (the tissue sample with a mucoadhesive fluorescent material applied on it before the start of first washing; this was considered as the zero time point with 100 % fluorescence intensity); and  $I$  represents the fluorescence intensity of that tissue sample with the mucoadhesive fluorescent material after each washing cycle. These fluorescence intensities were then converted into % mucosal retention values.

## 3. Results and discussion

To evaluate the suitability of thermoresponsive engineered emulsion formulations for nasal drug delivery systems, drug solubility tests were

conducted. Emulsions, consisting of dodecane in water (1:1) as shown in Fig. 1, were formulated using the optimal BCS identified in our previous work (Rajbanshi et al., 2023a, b). Two formulations were tested: one containing 10 wt% BCS alone and another with 10 wt% BCS combined with 0.25 wt% methylcellulose (MC). A range of drugs were explored and three drugs (phenylephrine hydrochloride, lidocaine hydrochloride and budesonide) were selected with respect to their range of solubility and partition coefficients covered (Table 2) (VCCLAB, 2023).

Emulsions were formulated with 0.5 wt% phenylephrine HCl, 5 wt% lidocaine HCl and 0.064 wt% budesonide to match reference licensed products (Martindale Pharma an Ethypharm Group Company, 2017; Sandoz Limited, 2022). The solubility and physical state of the drugs were carefully considered during emulsion formulation. Both phenylephrine and lidocaine in their salt forms, which are highly soluble in water, were dissolved in the aqueous phase and emulsified. However, budesonide, being highly insoluble in water, was suspended in the aqueous polymer solution before emulsification giving a cloudy dispersion of the drug. All mixtures successfully formed emulsions (Table 3), however degrees of creaming varied and hence so did emulsion yield in the BCS-stabilised systems. The various amounts of drugs added to the emulsion system increased the viscosity of the continuous phase thus reducing the velocities of the oil droplets to creaming. The addition of methylcellulose removed creaming in all systems. It has been reported in our previous studies that emulsions with BCS/MC contains droplets with small median diameters and narrower size distributions, contributing to the stability of the system (Rajbanshi et al., 2023a, b).

### 3.1. Emulsion characterisation

To examine the bulk properties of the emulsions further, rheological analyses of the BCS and BCS/MC stabilised drug-loaded emulsions were conducted (Fig. 2). The impact of temperature on the emulsions was evaluated by using small-amplitude oscillatory rheology at a fixed frequency. This experiment determined the storage ( $G'$ ) and loss ( $G''$ ) moduli within the linear viscoelastic range of the system (at a shear strain of 0.1 %), thus preserving the sample structure.

For BCS drug-loaded emulsions, the temperature ramp revealed distinct thermoresponsive behaviour (Fig. 3). At low temperatures, both

**Table 3**

Yield and oil phase volumes ( $\phi_{oil}$ ) of emulsions with BCS and BCS/MC; and drug-loaded emulsions with BCS and BCS/MC after isolation of the creamed phases at 36 h ( $n = 1$ ).

Emulsion	Yield (%)		$\phi_{oil}$	
	with BCS	with BCS/MC	with BCS	with BCS/MC
without drug	76	100	0.72	0.57
0.5 wt% Phenylephrine	80	100	0.65	0.57
5 wt% Lidocaine	86	100	0.74	0.57
0.064 wt% Budesonide	80	100	0.65	0.57

$G'$  and  $G''$  remained low, approximately 3 Pa for budesonide emulsion, 8 Pa for lidocaine emulsion and 15 Pa for phenylephrine emulsion. This indicated a predominantly liquid-like state for the lidocaine and budesonide emulsions ( $G'' > G'$ ). The phenylephrine emulsion behaved differently, as a thick viscoelastic liquid, with  $G'$  slightly greater than  $G''$ . As the temperature increased above around 30 °C, both moduli for all emulsions exhibited an increase, with a shift towards a more elastic character in the system. At 32 °C the system transitioned to a predominantly elastic state ( $G' > G''$ ). At this temperature, designated as  $T_{gel}$ , the formation of a gel-like structure was observed. This change is triggered by the lower critical solution temperature (LCST) of DEGMA, known to be around 31–35 °C when copolymerised with PEGMA (Rajbanshi et al., 2023a, b). Above  $T_{gel}$ , the systems reached a plateau at approximately 35 °C, with  $G'$  reaching close to 100 Pa in all examples. With further heating, both  $G'$  and  $G''$  decreased, likely due to reduced internal friction as more kinetic energy was added to the system or structural changes in the BCS system at higher temperatures.

Thermoresponsive behaviour was also observed in the BCS-MC drug-loaded emulsions. At low temperatures, both  $G'$  and  $G''$  remained low for budesonide and lidocaine, ranging from approximately 5 to 15 Pa indicating a predominantly liquid-like state ( $G'' > G'$ ). As with the BCS emulsions, the phenylephrine emulsion system demonstrated slightly more solid-like behaviour with  $G'$  over  $G''$ .  $T_{gel}$  for each emulsion was found to be 30 °C. Above this temperature, the budesonide and lidocaine emulsion reached  $G'$  of around 200 Pa. For the phenylephrine emulsion system, a plateau was observed at ca 120 Pa.

To assess the possibility of macroscopic instability events, all emulsions were left on the bench top without any disturbance under ambient conditions. Emulsions formulated with phenylephrine and budesonide were found to be stable with no further creaming after 36 h. After 10 days, it was observed that the lidocaine emulsions separated into 2 phase systems indicating breaking. Hence, a set of lidocaine emulsions stabilised by BCS and BCS/MC were prepared for stability studies. After 7 days of isolation, rheological analysis was conducted (Fig. 3). At low temperatures,  $G'$  was observed to be 10-fold greater (approximately 80 Pa) as compared to the emulsions analysed after 36 h of isolation (Fig. 3). As the temperature increased, a reduction in viscosity was observed leading to emulsion breaking at approximately 28 °C. Compared to the other drug-loaded emulsion systems, the lidocaine emulsions were formulated with the highest drug concentration (5 wt %). The higher drug content likely had both charge and steric impacts, hindering the BCS from connecting from one O/W interface, through the bulk, to another. This may have resulted in the displacement of BCS from the interface, concurrently altering the surface properties. Additionally, lidocaine is known to have intrinsic surface activity and thus may have anchored to the O/W interface (Sarheed et al., 2020).

Laser diffraction was used to measure droplet size distributions, giving  $X_{10}$ ,  $X_{50}$ , and  $X_{90}$  values (Table 4). Typically,  $X_{50}$ , representing the median is used as an average with the other two values giving a numerical description of dispersity.

Median particle size ( $X_{50}$ ) of all BCS drug-loaded emulsions demonstrated bimodal distributions when loaded with budesonide and

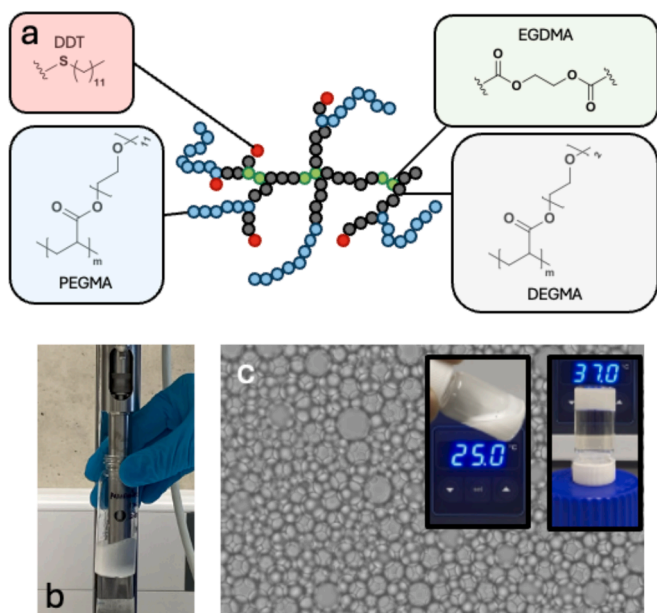


**Fig. 1.** Chemical structure and schematic of BCS (a), emulsion formulation with high shear homogenisation (b), light microscopy images at 20x magnification of dodecane in water (1:1) emulsion and its solution (25 °C) to gel (37 °C) transition without any syneresis observed (c).

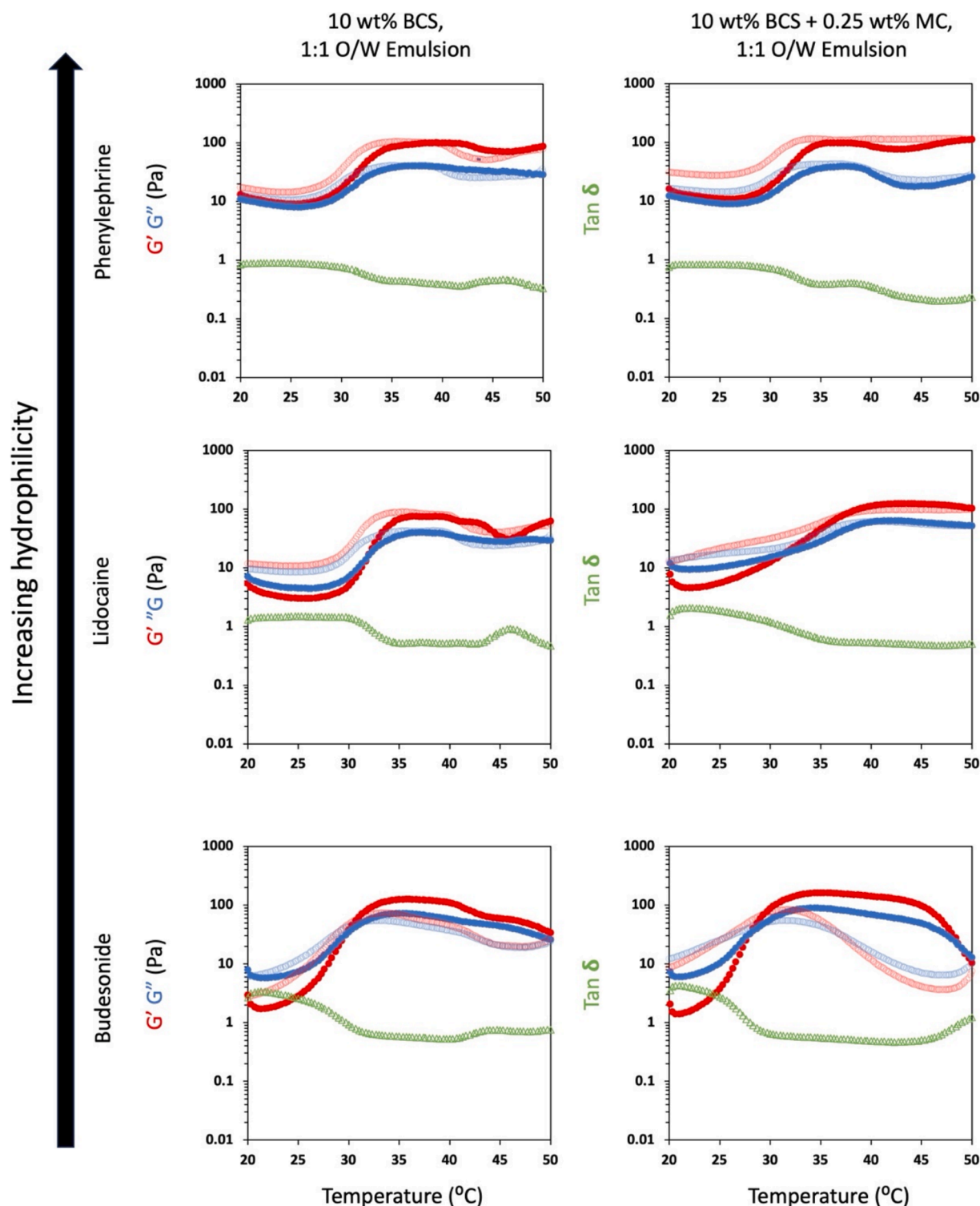


Fig. 2. Temperature-ramp oscillatory shear rheology of 1:1 o/w drug-loaded emulsions stabilised with 10 wt% BCS (left column), and drug-loaded emulsions stabilised with 0.25 wt% methylcellulose and 10 wt% BCS (right column).  $G'$  (red),  $G''$  (blue) and  $\tan \delta$  (green) are shown. Closed symbols indicate heating, whilst open symbols indicate cooling. The rheological measurements were conducted after 36 h of isolation. Rheological studies of control systems (emulsion with BCS and BCS/MC without drug) can be found in our previous work (Rajbanshi et al., 2023a, b).

lidocaine. For phenylephrine emulsions the distributions were largely monomodal with a minor shoulder at lower diameters (Fig. 4). The similarity in droplet size for all systems could be due to the same homogenisation technique used for the formation of droplet diameter (Table 4). Comparatively, the BCS-MC drug-loaded emulsions had smaller median droplet diameters and narrower distributions (Table 4

and Fig. 4). This is likely to contribute to the stability of the systems.

### 3.2. Drug loading and quantification

1 wt%, 10 wt% and 0.128 wt%, respectively, of phenylephrine, lidocaine and budesonide were added to aqueous BCS and BCS/MC



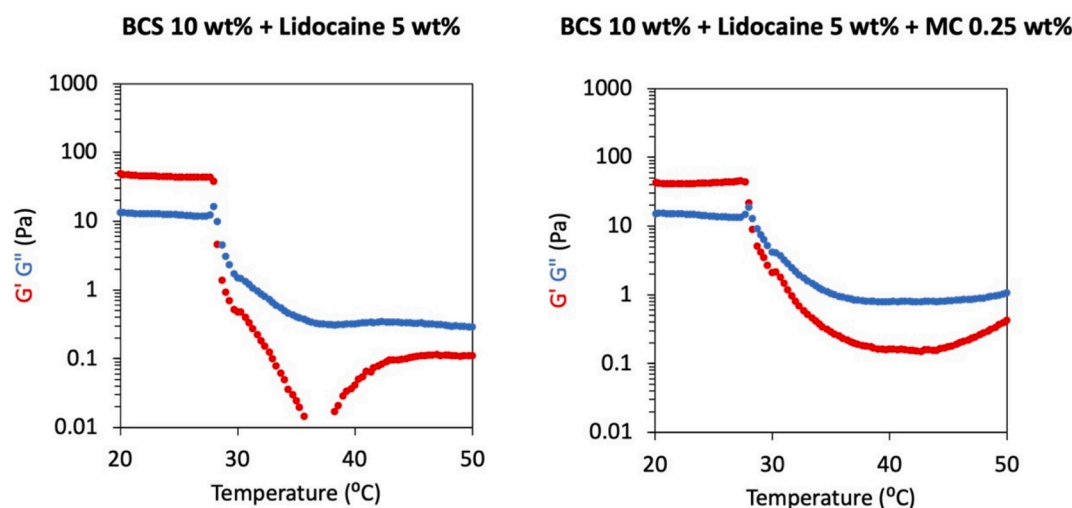


**Fig. 3.** Temperature-ramp shear rheology of 1:1o/w lidocaine loaded emulsions stabilised with 10 wt% BCS (left) and drug-loaded emulsions with 0.25 wt% methylcellulose and 10 wt% BCS (right) after 7 days storage at room temperature.  $G'$  (red) and  $G''$  (blue) are shown. The rheological analysis of the emulsion was conducted after 7 days of isolation.

**Table 4**

Droplet size of BCS and BCS/MC drug-loaded emulsions after isolation of the creamed phase for 36 h.

Droplet size ( $\mu\text{m}$ )	Phenylephrine		Lidocaine		Budesonide	
	Emulsion with BCS	Emulsion with BCS/MC	Emulsion with BCS	Emulsion with BCS/MC	Emulsion with BCS	Emulsion with BCS/MC
X10	1.30	2.09	1.38	1.82	1.26	2.00
X50	4.80	3.94	4.70	2.91	4.83	2.86
X90	9.51	6.85	10.21	4.29	10.46	3.90

solutions and emulsified with equal weight of dodecane oil phase. The resulting emulsions therefore contained a drug loading of 0.5 wt%, 5 wt % and 0.064 wt% of phenylephrine, lidocaine and budesonide, respectively, to match licensed formulations. Upon quantification, the drug loading of each 5 g of formulation (as % of the nominal content) for BCS emulsions was determined to be 81.5 % (20.375 mg) for phenylephrine, 91 % (227.5 mg) for lidocaine and 38.1 % (1.22 mg) for budesonide. Drug loading for BCS/MS emulsions was found to be 98 % (24.5 mg) for phenylephrine, 96 % (240.0 mg) for lidocaine and 51.3 % (1.64 mg) for budesonide (Table 5). In the budesonide formulation, drug was added as a suspension due to its low solubility, giving rise to the lower loading efficiency reported. The systems were not buffered which could be considered for weakly acidic or basic drugs

### 3.3. Drug release profiling using Franz diffusion cells

For phenylephrine drug release, 0.5 g of emulsion (2.5 mg phenylephrine) was added to the donor chamber of the Franz cell. The receiver fluid was PBS and sampling was conducted at time intervals of 0.25, 0.5, 1, 3, 6, 9, 12 and 24 h. The quantification of drug release in the receiver fluid was performed using HPLC analysis. Lidocaine-phenylephrine topical solution containing 5 %w/v solution of lidocaine and 0.5 %w/v solution of phenylephrine was used for comparison (Martindale Pharma an Ethypharm Group Company, 2017).

The cumulative release of phenylephrine formulated into either BCS or BCS/MC emulsions, as well as the reference product, was studied across a cellulose membrane over 24 h period (Fig. 5). The drug release profile of the commercially available topical solution gave relatively rapid liberation. It was observed that 60 % of drug was released after 1.5 h and over 80 % of the drug was released after 3 h. Both the BCS and BCS/MC emulsion systems retarded liberation across the membrane significantly, compared to the marketed solution products. In the BCS emulsion, it was observed that 60 % of the drug was released after 10 h

and 88 % of the drug was released after 24 h. The BCS/MS emulsion showed a further reduction in drug release rate, only liberating 60 % after 20 h and 65 % after 24 h.

Statistical evaluation of the drug release data was conducted using 2-way ANOVA with Bonferroni post-hoc testing for multiple comparisons. At 0 min, the release of phenylephrine from the reference sample and the BCS and BCS/MS emulsions was 0 %, as expected. At 15 min, drug release from the BCS emulsion and BCS/MC emulsion were significantly not different ( $p > 0.05$ ) with release below 5 % while the drug release from both the emulsion formulations were significantly different as compared to the reference product which showed a release of 11.1 %. Furthermore, except for these time points, in all the sampling events there were significant differences in release between all three formulations ( $p < 0.001$ ). The drug release pattern for both emulsion formulations showed controlled release relative to the reference product. The reference product showed more than 83 % after 3 h and 95.9 % release after 24 h, whereas the emulsions only reached 88 % (BCS) and 65 % (BCS/MS) release by 24 h.

For lidocaine drug release, 0.5 g of the emulsion (25 mg lidocaine) was added to the Franz cell donor compartment and PBS was added to the receiver chamber. The quantity of lidocaine permeated across the membrane from the BCS, BCS/MS emulsions and the reference product over a 24 h period was recorded (Fig. 5). Initially, at 0 h, all samples showed 0 % release. After 15 min, the BCS and BCS/MS emulsions showed <5 % release ( $p > 0.05$ ), significantly different to the reference product (10.4 %,  $p < 0.001$ ). After 30 min the emulsions showed <10 % release, whereas the reference showed 20.5 % ( $p < 0.001$ ). All subsequent time points continued to show significant differences in release between the emulsions and the reference ( $p < 0.001$ ). After 15 h the BCS emulsion, had released 60 % of the drug and after 24 h, 76 % was released. For the BCS/MC emulsion release was found to be 60 % after 21 h and 64.5 % after 24 h. Comparatively, the reference product released 60 % of the drug after 2 h and 91.4 % by 24 h. The lidocaine

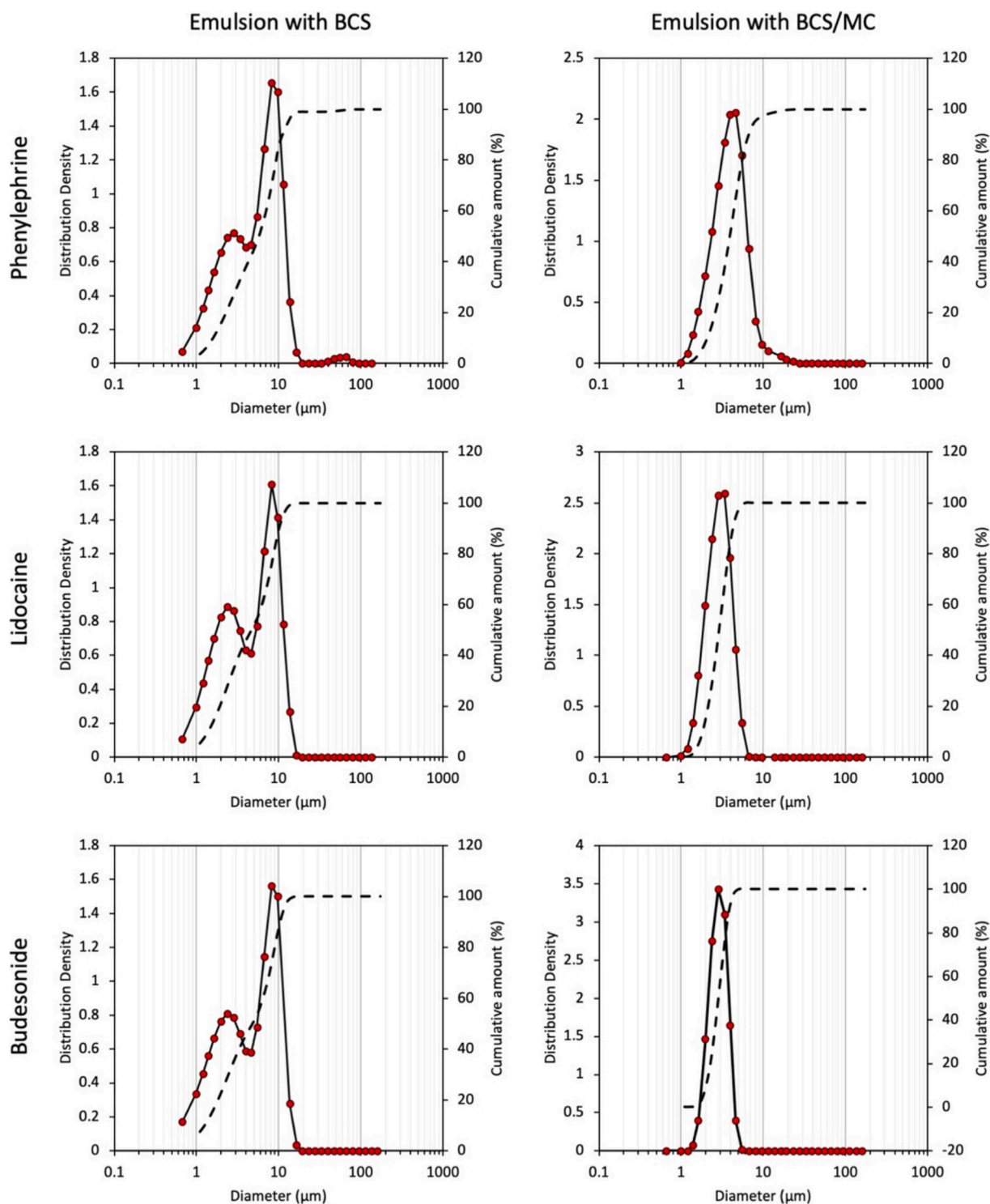


**Fig. 4.** Droplet size distribution of BCS drug-loaded emulsions (left column) and BCS/MS drug-loaded (right column) as determined by laser diffraction. Red points with solid line indicate distribution density, dotted lines indicate cumulative distribution.

release pattern was similar to phenylephrine, but with reduced rate (Fig. 5).

The cumulative amount of budesonide permeated across the membrane over 24 h period was also studied (Fig. 5). In the donor chamber of the Franz cell, 0.1 g of the emulsion (32  $\mu$ g budesonide) was added, in the receiver chamber a 0.2 %v/v solution of Tween-20 in PBS was used, determined by a preliminary solubility study (supplementary information, Fig. S5). It was observed that 60 % of the drug (calculated relative to the drug loading) was released in 9.5 h and 74 % of the drug was

released by 24 h. The BCS/MC emulsion showed drug release of 60 % after 12 h and 67.5 % after 24 h. Interestingly, the budesonide formulations showed near zero-order liberation for the first 9 h of the experiment. The reference product was found to release 60 % of the drug after 2 h and 83.9 % after 24 h.

The Korsmeyer-Peppas (Korsmeyer et al., 1983) equation was fitted to the drug release data to probe further the drug release kinetics from the BCS and BCS/MC emulsions (Section 2.5). Using the Korsmeyer-Peppas model, nonlinear curve fits were applied to the experimental



**Table 5**

Drug loading and quantification in 5 g of each BCS and BCS/MS emulsion systems ( $n = 6$ ). Drug loading percentage was calculated with respect to the amount of drug loaded in the system before emulsification.

Drug	Drug loaded (mg)	Drug quantified for emulsion with BCS		Drug quantified for emulsion with BCS/MC	
		in %	in mg	in %	in mg
Phenylephrine	25.0	81.5	20.38	98.0	24.50
Lidocaine	250.0	91.0	227.50	96.0	240.00
Budesonide	3.2	38.1	1.22	51.3	1.64

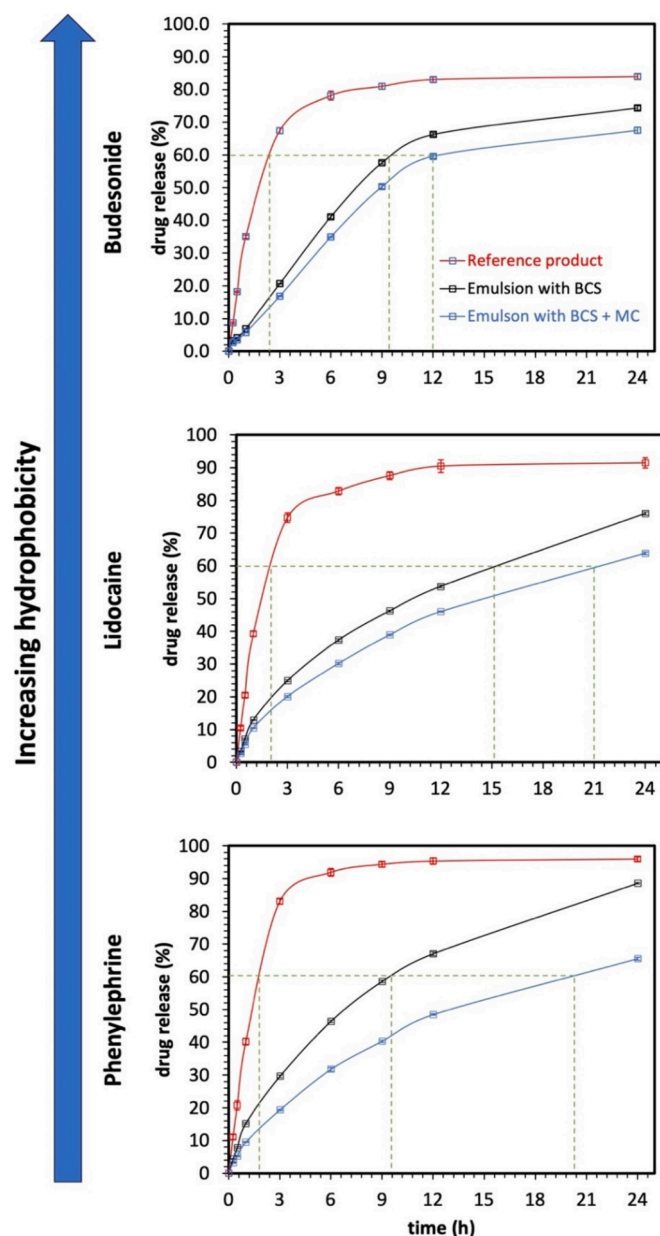


**Fig. 5.** Drug release profile of phenylephrine, lidocaine and budesonide from reference products, BCS emulsions, and BCS/MS emulsions using Franz diffusion cells ( $n = 6$ ).

data for the phenylephrine and lidocaine formulations and zero-order release kinetics were applied for the budesonide formulations (Fig. 6). The release constant ( $k$ ) is directly proportional to the diffusion constant and hence depends on the physical and structural properties of both the

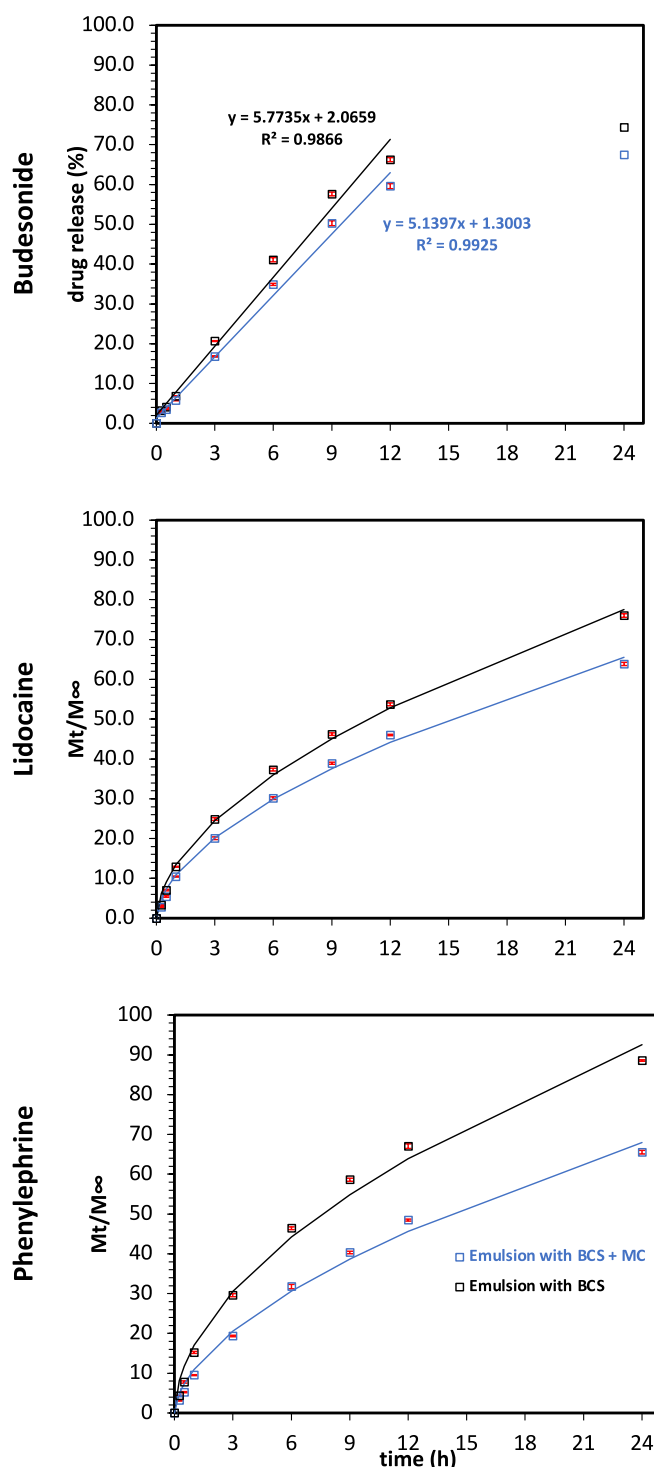


**Fig. 6.** Drug release profile fitted with Korsmeyer-Peppas model fit for phenylephrine and lidocaine emulsions; and zero-order kinetic model for budesonide emulsions. Solid lines represent the predicted model.

drug and BCS. The value of  $k$  is higher for the BCS-emulsions compared to the BCS/MS emulsions (Table 6). The  $n$  value is observed to be greater than 0.5 for all the systems, which is attributed to anomalous (non-Fickian) transport through the dialysis membrane, indicating that the dosage form affected liberation from the formulation system (Korsmeyer et al., 1983). The kinetic parameters obtained from the in vitro drug release data showed that the release of phenylephrine and lidocaine followed the diffusion model of Korsmeyer-Peppas (Table 6). The

**Table 6**

Parameters obtained from fitting the Korsmeyer-Peppas model to experimental data.

Korsmeyer-Peppas fit parameters	Phenylephrine		Lidocaine		Budesonide	
	Emulsion with BCS	Emulsion with BCS/MC	Emulsion with BCS	Emulsion with BCS/MC	Emulsion with BCS	Emulsion with BCS/MC
K	17	10.94	13.35	10.81	14.24	11.91
n	0.53	0.57	0.55	0.57	0.56	0.58
R <sup>2</sup>	0.9955	0.9969	0.9985	0.9982	0.9737	0.9749

correlation coefficient values ( $R^2$ ) were 0.9955 and 0.9969 for the phenylephrine BCS and BCS/MC emulsions respectively and 0.9985 and 0.9982 for the lidocaine BCS and BCS/MC emulsions respectively. For budesonide-loaded emulsions, the drug release obeyed zero order kinetics with  $R^2$  values of 0.9866 and 0.9925 for the BCS and BCS/MC emulsions, respectively. This may be due to higher affinity of the hydrophobic budesonide for the oil droplet, resulting in a zero-order release profile due to the requirement to partition from the oil into the external water phase prior to drug release from the formulation. Furthermore, the better fit with zero order kinetics was confirmed by assessing the correlation coefficient between the experimental and fitted values obtained through mathematical methodologies at various time points during the experimental duration. Mechanistically, zero order delivery can be achieved when the rate of partition of drug from oil to water is approximately equal to that rate of diffusion across the membrane from the water phase.

Overall, slower release is observed from the BCS/MC emulsions when compared to BCS emulsions and the reference products (Fig. 5). In BCS emulsions, the drug release may be controlled by multiple factors, including the drug's affinity for the BCS, its solubility in the oil phase, its diffusion through the BCS matrix, and the emulsion droplet size which can alter both the area of the O/W interface and the tortuosity of the aqueous inter-droplet space (Calderó et al., 1997, 2000). However, in the BCS/MC thermoresponsive gelation system, an additional factor is introduced. Methylcellulose is a hydrophilic polymer which forms a gel-like matrix when hydrated, which is known to slow down the dissolution and diffusion of a drug through the matrix (Calderó et al., 2000; Dewan et al., 2015). The addition of the MC therefore results in delayed drug release, as the drug molecules must diffuse through polymer networks before being released into the surrounding environment. The enhanced thermogelation strength of the emulsion, as evidenced by the rheology studies (section 3.1) could have also contributed to the delayed release. A stronger gel matrix can impede drug diffusion, leading to a slower release rate. Hence, the differences in drug release rate from BCS and BCS/MC systems can be attributed to the interplay between drug-polymer interactions and the influence of the MC hydrated layer on these interactions.

A slower release was observed with BCS/MC formulation despite the emulsion droplet size being smaller when compared to the formulation with only BCS (Table 4, Fig. 4). Conventionally, smaller emulsion droplets are generally associated with a greater surface area of the oil, potentially leading to an accelerated drug release from oil to water (Calderó et al., 1997). Hence, the polymer in the bulk or at the interface is believed to be limiting the release rate. The drug release patterns for phenylephrine, lidocaine, and budesonide showed that phenylephrine is released the fastest. After 24 h, drug release from the BCS-emulsions was 89 % for phenylephrine, 76 % for lidocaine, and 74 % for budesonide. For the BCS/MS-emulsions, release was 66 %, 64 % and 68 %, respectively. The difference in release corresponds to the hydrophobicity of the drugs. Phenylephrine, the least hydrophobic, has a higher affinity for the water phase than the oil phase, leading to quicker release. Lidocaine, which is more hydrophobic, is released at an intermediate rate as it slowly partitions from the oil phase to the surrounding medium. Budesonide, the most hydrophobic, remains primarily in the oil phase, resulting in the slowest release.

The release pattern was also related to how the drugs diffuse through

a medium. Hydrophobic drugs can interact with the oil phase of the emulsion or polymer surfactants, slowing diffusion (Calderó et al., 1997, 2000). Additionally, polymer micelles, present in the aqueous phase, can interact with hydrophobic drugs (Babak, Stébé and Fa, 2003). This further slows their release from the emulsion, as they must diffuse out of the micelle first. Tortuosity within the polymer matrix and oil droplets can also affect the drug release. Budesonide, being the most hydrophobic, is likely to encounter more tortuous paths, resulting in slower release compared to lidocaine and phenylephrine. The interaction of the drug with the gel structure, and diffusion through the thermogelling systems likely also influenced the release mechanisms.

### 3.4. Drug delivery platform and nasal spray device assembly

Thermoresponsive engineered emulsions hold great potential as drug delivery vehicles for nasal application. The low viscosity at room temperature should allow the material to be sprayed effectively. Post-spraying, a thermoresponsive switch to a gel state, stimulated by the nasal temperature, should allow the material to better resist shear and enhance retention. The delivery of highly-viscous solutions necessary to achieve mucoadhesion (Smart, 2005) has long been regarded as a challenge for traditional nasal sprays designs that achieve shear of  $10^5$ – $10^6$  s<sup>-1</sup>, with a viscosity limit of ~0.02–0.03 Pa s prevents uniform dispersion of a droplet aerosol cloud (Dayal, Shaik and Singh, 2004). As such, the emulsions developed in this project were evaluated for compatibility with a novel spray device (NasaDose) (Recipharm, 2023) developed by Bepak Ltd. NasaDose is a unit dose nasal spray device, designed to have user-independent actuation and spray performance. This means that it delivers intranasal formulations repeatably and reliably, as per essential performance requirements outlined in the FDA guidance for nasal sprays, regardless of the force applied by the user to actuate it. This has been demonstrated previously with different formulations, including sumatriptan (active), a low viscosity placebo and 20 cP silicone oil. The samples provided for this study were “off the shelf” devices with the standard NasaDose configuration and had not been optimised for delivery of the emulsion under investigation.

To test the suitability of the device, atomisation and qualitative tests were performed. In each test, the emulsion was added to the vial of the NasaDose (Recipharm, 2023) nasal spray device and droplet size distribution (DSD), plume geometry, spray pattern and shot weights were determined (Fig. 7).

### 3.5. Determination of shot weights

The determination of shot weights serves to verify valve functionality and assess pump-to-pump consistency for accurate and reproducible dosing (FDA, 2002; Farina, 2010). To determine shot weights from the NasaDose nasal spray, devices were weighed before and after each actuation using an analytical balance. Our investigation examined for any relationship between the actuation force and shot weight (Fig. 8). After the actuation of 45 devices (each using 0.1 g emulsion), the average dispensed dose was found to be  $52.5 \pm 3.6$  mg, with an average actuation force of  $32.6 \pm 2.6$  N. The device demonstrates independence of actuation force and dose, expected by the spring design. Despite the formulations lying outside the typically accepted range of viscosities for nasal spray actuation, the average performance with the



Fig. 7. Atomisation of engineered emulsions stabilised with 10 wt% BCS through unit dose nasal device (NasaDose) (Recipharm, 2023).

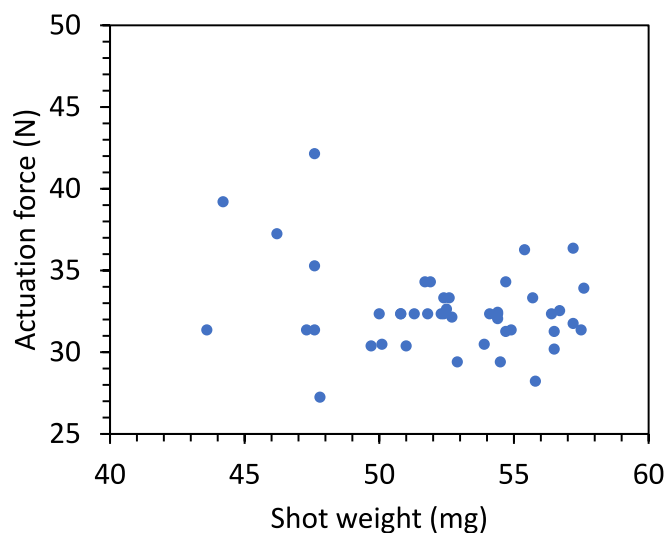


Fig. 8. Impact of actuation force on shot weight using the NasaDose nasal device (45 actuations).

NasaDose device was acceptable. Nevertheless, several outliers were outside the  $\pm 15\%$  regulatory limit (FDA, 2002), identifying the need for formulation-device optimisation. Thus, the device and formulation parameters will require optimisation if adopted for medical use. Parameters that may be considered to reduce deviations include viscosity, surface tension, actuation stroke length, force and velocity (Trows et al., 2014).

### 3.6. Droplet size distribution (DSD)

The DSD within the nasal spray is a critical parameter to assess how the drug is deposited within the nasal cavity during in vivo

administration. The dimensions of these droplets are primarily influenced by several factors such as the design of the nasal device, actuation force, actuation velocity, stroke length, the distance between the nozzle and the laser beam, spraying angle and the viscosity and surface tension of the formulation (Trows et al., 2014). Laser diffraction was used to measure the size of droplets in real time. The droplet sizes of a single spray were measured at both 3 and 6 cm distances from the nozzle tip (Table 7). The data were collected during the fully developed phase of the spray and the sizes are expressed as  $D_{10}$ ,  $D_{50}$ ,  $D_{90}$  as well as span. The measurement distances were found to influence  $D_{10}$ ,  $D_{50}$  and  $D_{90}$  due to the evolution of a spray plume. The average median droplet size ( $D_{50}$ ) was found to be  $186\ \mu\text{m}$  for 3 cm and  $197\ \mu\text{m}$  for 6 cm. There was a slight effect on span with an average of 1.515 and 1.584 for measurement distances of 3 cm and 6 cm respectively. The acceptance criteria for the median droplet size falls within the range of  $30\text{--}120\ \mu\text{m}$  (FDA, 2002). When droplets are above  $120\ \mu\text{m}$ , they tend to deposit in the anterior regions of the nasal passage whereas if the droplets are less than  $10\ \mu\text{m}$ , they could potentially be inhaled reaching the lungs and causing adverse effects. The formulations show a desirable droplet size distribution with negligible fine fraction ( $<10\ \mu\text{m}$ ) (Table 7). Some variability was observed in the DSD; however this may have occurred due to the emulsion viscosity, the nozzle size and the nasal device parameters. Although the median droplet diameter was larger than desired with these formulations, given that  $0.02\ \text{Pa s}$  has been reported to be the maximum viscosity enabling the production of acceptable droplet sizes (Pennington et al., 2008), it is all the more remarkable that aerosol droplets were produced for the BCS formulations with the NasaDose device, and provides excellent potential for a formulation-device optimization in our future work.

### 3.7. Plume geometry and spray pattern

For optimal deposition in the nasal cavity, the plume angle needs to be carefully controlled. A plume angle that is too narrow may result in the spray being directed too high in the nostrils, potentially missing the targeted areas within the nasal passages. A plume angle that is too wide might cause the spray to impact the nasal septum or even exit the nasal cavity altogether (Gao, Shen and Mao, 2020). To effectively deposit the spray in the desired regions of the nasal cavity, the plume angle should be adjusted to align with the anatomy and airflow patterns within the nose. This ensures that the spray particles are carried by the nasal airflow to the intended target areas, such as the nasal cavity and the mucosal surfaces, where efficient absorption can occur. Hence, the plume angle of a nasal spray is one of the critical parameters for optimal therapeutic effect. Trows et al. investigated the influence of viscosity and suggested that a decrease in plume angle and spray area were observed with an increase in the viscosity of the formulation (Trows et al., 2014). Moreover, the plume geometry can also be affected by the type of nozzle, measurement distance and actuation force. For the determination of plume geometry, a laser sheet and high-speed digital camera were used. Images were taken from a sideward view of the emitted spray parallel to the axis of the plume (Fig. 9). Plume angles were determined to be from  $51.1^\circ$  to  $23.1^\circ$ , and plume widths were found to be between  $28.71\ \text{mm}$  to  $12.25\ \text{mm}$  (measured at 6 cm from nozzle) (Table 8). The average plume angle of  $38^\circ$  suggests potential efficient delivery to the turbinate region of the nasal mucosa. Previous studies have shown that formulations with a similar plume angle can deliver 80 % of the dose to this region (Foo et al., 2007). This highly vascularised and permeable region of the nasal cavity is ideal for systemic drug delivery.

To assess the spray pattern, an image capturing a cross-sectional view of the plume along the axial direction was employed at 3 and 6 cm from the actuator tip (Table 7). The plume width data supplements the spray pattern data and was determined based on single actuation. Spray patterns measured at 3 cm showed variable results for the ovality ratio, ranging from 1.12 to 2.59. Whereas, at 6 cm no significant changes

**Table 7**  
The droplet size distribution and span measured at 3 and 6 cm from the nozzle.

Actuations	Droplet Size Distribution @ 3 cm (µm)					Droplet Size Distribution @ 6 cm (µm)				
	%<10 µm	D <sub>10</sub>	DV <sub>50</sub>	DV <sub>90</sub>	Span	%<10 µm	DV <sub>10</sub>	DV <sub>50</sub>	DV <sub>90</sub>	Span
1	0.00	70.23	160.60	313.60	1.52	0.00	40.89	88.49	181.00	1.58
2	0.00	35.88	90.87	183.60	1.63	0.00	339.70	511.40	744.00	0.79
3	0.00	64.20	147.10	287.60	1.52	0.00	51.68	148.10	309.50	1.74
4	0.00	242.40	459.80	759.90	1.13	0.17	47.00	122.80	257.50	1.71
5	0.00	38.64	99.73	207.20	1.69	0.00	82.12	172.10	316.20	1.36
6	0.00	123.50	267.50	558.70	1.63	0.00	31.18	71.56	169.70	1.94
7	0.00	71.17	163.20	318.20	1.51	0.00	81.90	202.50	420.20	1.67
8	0.00	87.53	181.60	340.60	1.39	0.00	37.76	90.86	196.30	1.75
9	0.00	59.17	152.80	306.80	1.62	0.00	39.21	95.98	203.80	1.72
10	0.00	58.49	138.30	269.50	1.53	0.14	274.20	468.40	755.40	1.03
Mean		85.12	186.15	354.57	1.52		102.56	197.22	355.36	1.53
SD		60.59	107.59	174.52	0.16		110.22	159.87	221.52	0.36

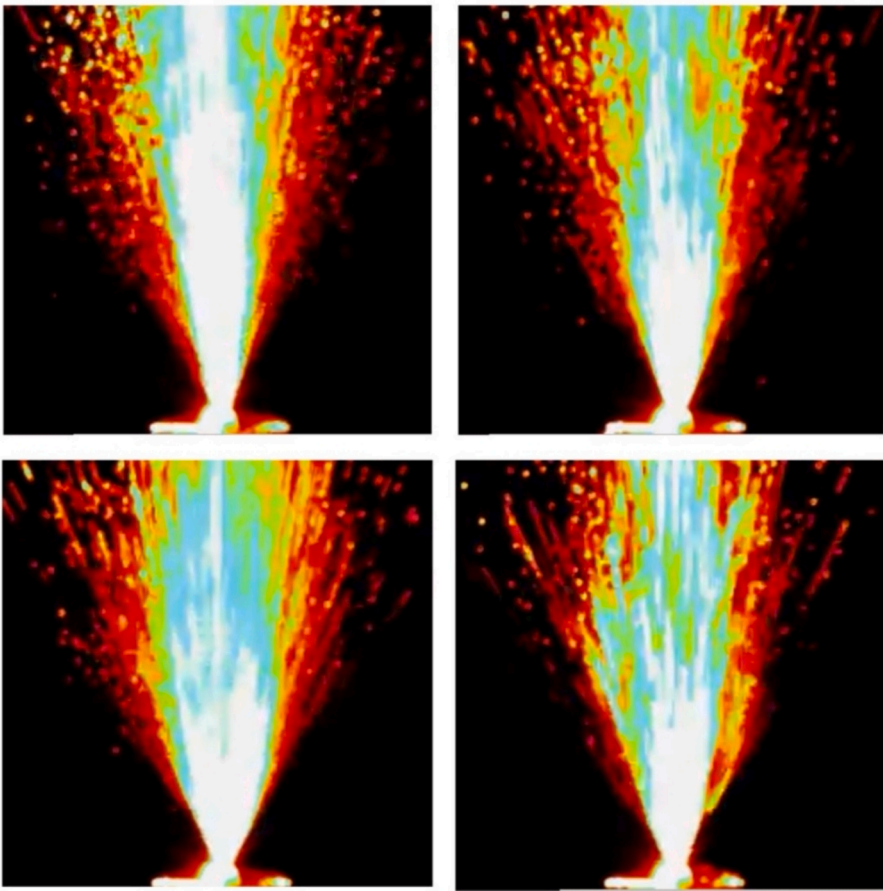


**Fig. 9.** Plume geometry and spray pattern from NasaDose nasal spray loaded with engineered emulsion stabilised with 10 wt% thermoresponsive BCS captured by a high-speed digital camera. Images captured of four devices actuated manually showing reproducibility with slight variations.

were observed in the ovality ratio. It should be noted that the spray pattern increases with increasing actuation velocity, leading to a slight decrease in spray pattern ovality (Newman et al., 1988). A spray pattern with low ovality (circular) is the most desirable as it ensures an even distribution of the spray within the nasal cavity. This enhances the effectiveness and consistency of drug delivery and absorption, contributing to the overall performance of the nasal spray for therapeutic outcomes (Gao, Shen and Mao, 2020). It is of note that ovality and spray area achieved with the NasaDose device for the thermogelling BCS emulsion were broadly in line with those achieved for low viscosity solutions (200–700 mm<sup>2</sup>) (Pennington et al., 2008), and that have been shown to be suitable for nose-brain drug delivery (Wingrove et al.,

2019). The studies performed on the BCS-emulsions in the nasal spray devices highlighted that the viscosity of the formulation is a critical factor. Viscosity significantly influenced DSD, shot weight, plume geometry and spray pattern. In future studies, it will be crucial to balance the BCS molecular weight and concentration, which enhance the stability of the emulsion and increase the magnitude of gelation, with the ideal viscosity for effective spray function.

3.8. In vitro cytotoxicity evaluation

Considering the potential for nasal application using a device,



**Table 8**

Evaluation of plume geometry 6 cm from the nasal spray device nozzle.

Actuations	Plume Geometry @ 6 cm		Spray Pattern @ 3 cm			Spray Pattern @ 6 cm		
	Plume Angle (°)	Plume Width (mm)	Dmax (mm)	Ovality	Area (mm <sup>2</sup> )	Dmax (mm)	Ovality	Area (mm <sup>2</sup> )
1	40.7	22.26	20.88	1.17	288.80	46.16	1.42	1142.50
2	46.1	25.65	22.61	1.15	347.10	34.40	1.33	662.80
3	23.1	12.25	19.09	1.27	222.50	36.17	1.35	722.80
4	29.3	15.70	16.15	2.59	74.70	29.13	1.35	474.90
5	51.1	28.71	18.91	1.25	228.10	32.10	1.29	596.40
6	45.1	24.89	21.88	1.86	191.50	36.31	1.32	813.90
7	32.7	17.61	22.28	1.12	343.50	45.99	1.24	1395.90
8	27.2	14.55	22.77	1.19	347.40	33.67	1.71	470.10
9	48.2	26.8						
Mean	38.2	20.20	20.57	1.45	255.45	36.74	1.38	784.91
SD	10.3	5.98	2.34	0.52	95.85	6.20	0.15	327.66

further assessment of the candidate formulations was performed using in vitro cell culture. Cytotoxicity was determined for the BCS in comparison to a known cytotoxic positive control (Triton-X) and benchmarked against surfactants which are already listed in the FDA's inactive ingredients database, namely sodium lauryl sulfate (SLS), Tween 20 (T20) and Tween 80 (T80). SLS is an anionic surfactant which appears in approved medicines at up to 65 % concentration and has been approved for routes of administration including topical and respiratory application. T20 and T80 are non-ionic polysorbates that appear in approved medicines at up to 15 % for routes of administration including injectables, topicals, and nasal medicines.

Cytotoxicity of these surfactants and BCS were performed on a human neuroblastoma cell line with neuron-like properties to represent the olfactory region of the nasal mucosa. The linear relationship between luminescence and SH-SY5Y cell number was confirmed using a CellTiter-Glo® assay (Fig. S1).

BCS showed a classical reverse sigmoidal dose-response ( $R^2 = 0.9772$ ), expressed as a percentage of a non-treated control and was compared to a known cytotoxic surfactant, Triton X-100 (Fig. 10A). The BCS concentration lethal to 50 % of cells ( $LC_{50}$ ), was determined as 0.662 mg/mL. A side-by-side comparison of cytotoxicity of the BCS and comparator surfactants is shown in Fig. 10B, with no significant differences in cell viability observed between materials at 0.2 mg/mL and below. BCS appears to be more cytotoxic than T20 and T80 at higher concentrations. Whilst in vitro cytotoxicity thresholds are not explicitly defined for medicinal products, ISO 10993-5 defines medical device cytotoxicity as the concentration when fewer than 70 % of the cells tested are viable. With this threshold in mind, SLS and BCS both exhibited cytotoxicity in vitro at approximately 0.2 mg/mL, giving a positive indicator of comparable tolerance.

### 3.9. Ex vivo mucoadhesion assessment

Mucoadhesion was assessed on ex vivo sheep nasal mucosa using a well-established flow-through method to give indicators of behaviours in vivo (Fig. 11) (Porfiryeva et al., 2019; Vanukuru et al., 2024). FITC-dextran and chitosan were used as controls to represent a known mucoadhesive and a polymer with low mucoadhesion, respectively. In these experiments, retention is evaluated qualitatively with image collection (Fig. 11i) and quantified by the pixel intensity of the image (Fig. 11ii). Visually, retention of the BCS-stabilised emulsion formulation was greater than the chitosan (1 wt%) and dextran (1 wt%) solution as controls (Fig. 11i). Quantitatively the rank order adhesion was BCS > Chitosan > FITC-dextran at the longest timepoint in the experiments. Chitosan is well-known for its excellent mucoadhesion, driven by electrostatics, hydrogen bonding, and hydrophobic interactions with the mucosa (Sogias, Williams and Khutoryanskiy, 2008; Sandri et al., 2012). At the end of the study the BCS emulsion exceeded the degree of retention of chitosan by ca 75 % (51 vs 29 % remaining, respectively). Factors which may make the emulsion system very retentive include the potential for hydrophobic interactions, a driver of adhesion (Cook et al., 2017), and the immiscibility of the oil phase with water, making the system resistant to wash-off. These ex vivo studies further indicate the great potential of the BCS-stabilised emulsions in the preparation of nasal medicines.

## 4. Conclusion

The exploration of thermoresponsive engineered emulsions for nasal delivery of small molecules was reported in this study. The emulsions were versatile and able to incorporate phenylephrine, lidocaine, and

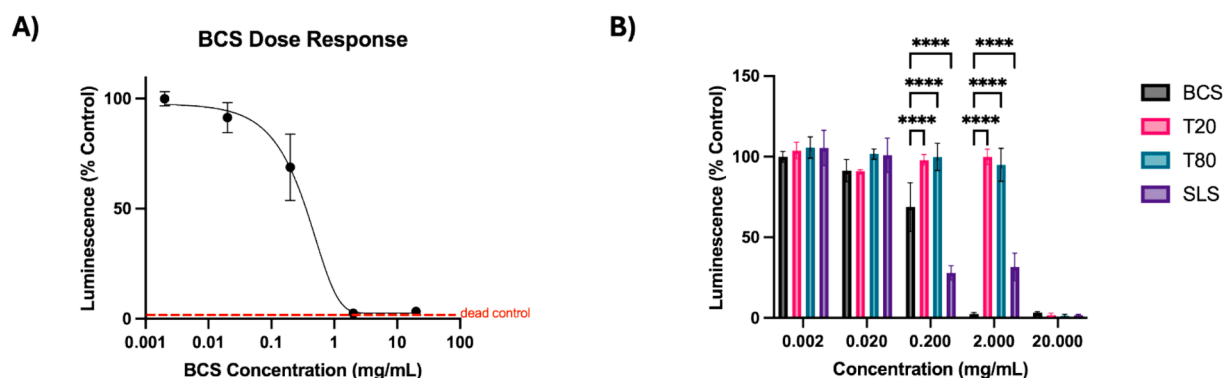


**Fig. 10.** Cytotoxicity of BCS, T20, T80, and SLS where the viability of SH-SY5Y human neuroblastoma cells was inferred using ATP concentration, measured using CellTiter-Glo®. Data were normalised as a percentage of a non-treated control and expressed as mean  $\pm$  SD ( $n = 3$  in triplicate independent experiments). A) Dose-response of BCS. B) BCS was compared to each of the other surfactants and significant differences are indicated where present at each concentration (two-way ANOVA with Tukey's multiple comparisons test, \*\*\*\*  $P < 0.0001$ ).

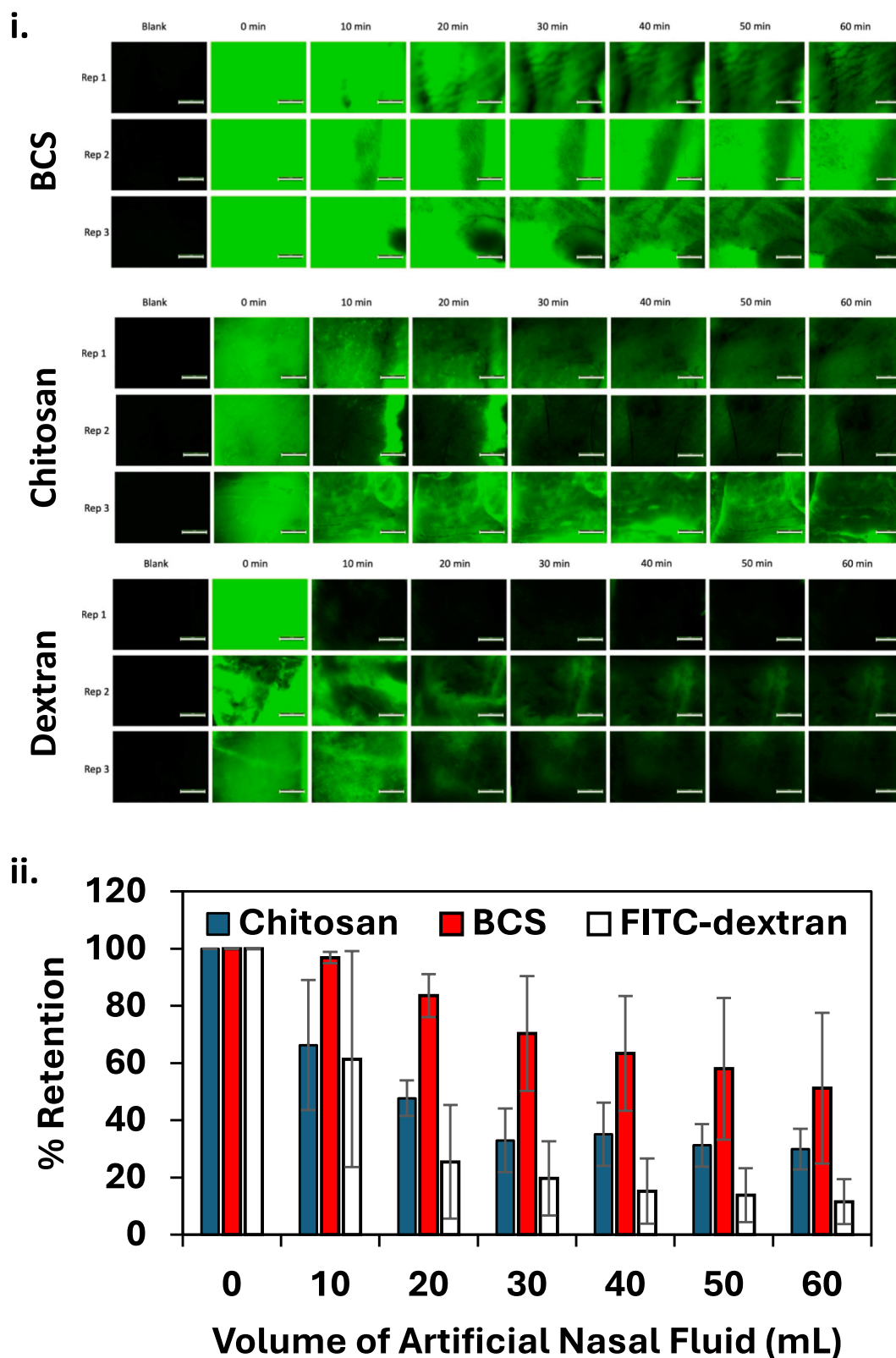


**Fig. 11.** Mucoadhesion assessment ex vivo on sheep nasal mucosa using a flow-through method. Images are collected of target formulations (i) and percentage retention is calculated as a function of volume of artificial nasal fluid flow (ii). Data presented as mean  $\pm$  standard deviation (N = 3).

budesonide drugs. The drug release was significantly retarded in the emulsions compared to a reference product available on the market. Liberation from the emulsion systems occurred over several hours, opening the possibility of sustained effects from nasal medicines.

Furthermore, ex vivo mucoadhesion assessment on sheep nasal mucosa indicated a significant retentive effect of the in situ gel-forming emulsion system, outperforming chitosan as a positive control. Taken together, this enhanced retention alongside controlled liberation



indicates a potential for extended delivery of drugs via the nose. To this end, compatibility of the system with a nasal spray device was assessed. It was found that the emulsions could be sprayed and successfully atomised by these systems, with exceedingly little fine fraction, and generating a spray plume with properties that are promising for nasal delivery. This indicates that nasal medicines developed from these systems may attenuate the fraction of inhaled dose from nasal sprays, as well as delivering emulsion to the nasal mucosa. Furthermore, evaluation of cytotoxicity was benchmarked the BCS excipient against common surfactants used as excipients, indicating a comparable cytotoxicity to SDS. Overall, this research provides valuable insights into the development and characterisation of thermoresponsive emulsions for drug delivery applications, offering potential new avenues for controlled delivery of active pharmaceutical agents through nasal routes.

## CRediT authorship contribution statement

**Abhishek Rajbanshi:** Writing – original draft, Validation, Resources, Project administration, Methodology, Investigation, Formal analysis, Data curation, Conceptualization. **Eleanor Hilton:** Writing – review & editing. **Emily Atkinson:** Methodology, Investigation. **James B. Phillips:** Writing – review & editing, Supervision. **Shiva Vanukuru:** Writing – review & editing, Methodology, Investigation. **Vitaliy V. Khutoryanskiy:** Writing – review & editing, Supervision. **Adam Gibbons:** Writing – review & editing, Validation, Software, Methodology, Investigation, Formal analysis, Data curation. **Sabrina Falloon:** Writing – review & editing, Validation, Software, Methodology, Investigation, Formal analysis, Data curation. **Cecile A. Dreiss:** Writing – review & editing, Supervision, Resources, Project administration, Funding acquisition, Conceptualization. **Darragh Murnane:** Writing – review & editing, Visualization, Supervision, Resources, Project administration, Funding acquisition, Conceptualization. **Michael T. Cook:** Writing – review & editing, Visualization, Validation, Supervision, Software, Resources, Project administration, Methodology, Investigation, Funding acquisition, Formal analysis, Data curation, Conceptualization.

## Declaration of competing interest

The authors declare that they have no known competing financial interests or personal relationships that could have appeared to influence the work reported in this paper.

## Appendix A. Supplementary data

Supplementary data to this article can be found online at <https://doi.org/10.1016/j.ijpharm.2025.125506>.

## Data availability

Data will be made available on request.

## References

- Babak, V.G., Stébé, M.J., Fa, N., 2003. Physico-chemical model for molecular diffusion from highly concentrated emulsions. *Mendelev Commun.* 13 (6), 254–256. <https://doi.org/10.1070/MC2003v013n06ABEH001794>.
- Bahadur, S., Pathak, K., 2012. Physicochemical and physiological considerations for efficient nose-to-brain targeting. *Expert Opin. Drug Deliv.* 9 (1), 19–31. <https://doi.org/10.1517/17425247.2012.636801>.
- Bhise, S., et al., 2008. Bioavailability of intranasal drug delivery system. *Asian J. Pharm.* 2 (4), 201. <https://doi.org/10.4103/0973-8398.45032>.
- Calderó, G., et al., 1997. Influence of composition variables on the molecular diffusion from highly concentrated water-in-oil emulsions (gel-emulsions). *Langmuir* 13 (3), 385–390. <https://doi.org/10.1021/la9603380>.
- Calderó, G., et al., 2000. Effect of pH on mandelic acid diffusion in water in oil highly concentrated emulsions (gel-emulsions). *Langmuir* 16 (4), 1668–1674. <https://doi.org/10.1021/la990971w>.
- Cook, S.L., et al., 2017. Mucoadhesion: A food perspective. *Food Hydrocoll.* 72, 281–296. <https://doi.org/10.1016/j.foodhyd.2017.05.043>.
- Costantino, H.R., et al., 2007. Intranasal delivery: Physicochemical and therapeutic aspects. *Int. J. Pharm.* 337 (1–2), 1–24. <https://doi.org/10.1016/j.ijpharm.2007.03.025>.
- da Silva, M.A., et al., 2022. Engineering Thermoresponsive Emulsions with Branched Copolymer Surfactants. *Macromol. Mater. Eng.* 307 (10), 1–14. <https://doi.org/10.1002/mame.202200321>.
- Dayal, P., Shaik, M.S., Singh, M., 2004. Evaluation of different parameters that affect droplet-size distribution from nasal sprays using the Malvern Spraytec®. *J. Pharm. Sci.* 93 (7), 1725–1742. <https://doi.org/10.1002/jps.20090>.
- Dewan, M., et al., 2015. Effect of methyl cellulose on gelation behavior and drug release from poloxamer based ophthalmic formulations. *Int. J. Biol. Macromol.* 72, 706–710. <https://doi.org/10.1016/j.ijbiomac.2014.09.021>.
- Ehrick, J.D., Shah, S.A., Shaw, C., Kulkarni, V.S., Coowanitwong, I., De, S., Suman, J.D., 2013. Considerations for the development of nasal dosage forms. Sterile Product Development: Formulation, Process, Quality and Regulatory Considerations 99–144. [https://doi.org/10.1007/978-1-4614-7978-9\\_5](https://doi.org/10.1007/978-1-4614-7978-9_5).
- Farina, D.J., 2010. Regulatory aspects of nasal and pulmonary spray drug products. In: Handbook of Non-Invasive Drug Delivery Systems. William Andrew Publishing, pp. 247–290. <https://doi.org/10.1016/b978-0-8155-2025-2.10010-1>.
- FDA, 2002. 'Nasal Spray and Inhalation Solution, Suspension, and Spray Drug Products — Chemistry, Manufacturing, and Controls', Final, (July), pp. 10–15. <https://www.fda.gov/media/70857/download>.
- Foo, M.Y., et al., 2007. The influence of spray properties on intranasal deposition. *J. Aerosol Med.: Deposit., Clearance, Effects Lung* 20 (4), 495–508. <https://doi.org/10.1089/jam.2007.0638>.
- Gao, M., Shen, X., Mao, S., 2020. Factors influencing drug deposition in the nasal cavity upon delivery via nasal sprays. *J. Pharm. Investig.* 50 (3), 251–259. <https://doi.org/10.1007/s40005-020-00482-z>.
- Harron, D.W.G., 2013. Technical Requirements for Registration of Pharmaceuticals for Human Use: The ICH Process. *Textbook Pharm. Med.* 447–460. <https://doi.org/10.1002/9781118532331.ch23>.
- ICH, 2022. 'ICH Harmonised Guidance: Validation of Analytical Procedures Q2(R2)', *ICH Harmonised Tripartite Guideline*, 2(March), pp. 1–34. [https://database.ich.org/sites/default/files/Q1A%28R2%29\\_Guideline.pdf](https://database.ich.org/sites/default/files/Q1A%28R2%29_Guideline.pdf).
- Illum, L., 2003. Nasal drug delivery - Possibilities, problems and solutions. *J. Control. Release* 87 (1–3), 187–198. [https://doi.org/10.1016/S0168-3659\(02\)00363-2](https://doi.org/10.1016/S0168-3659(02)00363-2).
- Kapoor, M., Cloyd, J.C., Siegel, R.A., 2016. A review of intranasal formulations for the treatment of seizure emergencies. *J. Control. Release* 237, 147–159. <https://doi.org/10.1016/j.jconrel.2016.07.001>.
- Korsmeyer, R.W., et al., 1983. Mechanisms of solute release from porous hydrophilic polymers. *Int. J. Pharm.* 15 (1), 25–35. [https://doi.org/10.1016/0378-5173\(83\)90064-9](https://doi.org/10.1016/0378-5173(83)90064-9).
- Lee, D., Minko, T., 2021. Nanotherapeutics for nose-to-brain drug delivery: An approach to bypass the blood brain barrier. *Pharmaceutics* 13 (12). <https://doi.org/10.3390/pharmaceutics13122049>.
- Leung, S.-H., Robinson, J.R., 1987. The contribution of anionic polymer structural features to mucoadhesion. *J. Control. Release* 5 (3), 223–231. [https://doi.org/10.1016/0168-3659\(88\)90021-1](https://doi.org/10.1016/0168-3659(88)90021-1).
- Martindale Pharma an Ethypharm Group Company, 2017. *Lidocaine Hydrochloride 5% w/v and Phenylephrine Hydrochloride 0.5% w/v Topical Solution*. <https://www.medicines.org.uk/emc/product/3592/smpc/print> (accessed: 16 August 2023).
- Moakes, R.J.A., et al., 2021. Formulation of a Composite Nasal Spray Enabling Enhanced Surface Coverage and Prophylaxis of SARS-COV-2. *Adv. Mater.* 33 (26). <https://doi.org/10.1002/adma.202008304>.
- Newman, S.P., Moren, F., Clarke, S.W., 1988. Deposition pattern of nasal sprays in man. *Rhinology* 26, 111–120.
- Ong, H.X., et al., 2016. Primary air-liquid interface culture of nasal epithelium for nasal drug delivery. *Mol. Pharm.* 13 (7), 2242–2252. <https://doi.org/10.1021/acs.molpharmaceut.5b00852>.
- Pennington, J., et al., 2008. Spray pattern and droplet size analyses for high-shear viscosity determination of aqueous suspension corticosteroid nasal sprays. *Drug Dev. Ind. Pharm.* 34 (9), 923–929. <https://doi.org/10.1080/03639040802149046>.
- Pires, P.C., et al., 2022. Strategies to Improve Drug Strength in Nasal Preparations for Brain Delivery of Low Aqueous Solubility Drugs. *Pharmaceutics* 14 (3), 1–18. <https://doi.org/10.3390/pharmaceutics14030588>.
- Porfiryeva, N.N., et al., 2019. Acrylated Eudragit® E PO as a novel polymeric excipient with enhanced mucoadhesive properties for application in nasal drug delivery. *Int. J. Pharm.* 562 (March), 241–248. <https://doi.org/10.1016/j.ijpharm.2019.03.027>.
- Pozzoli, M., et al., 2016. Application of RPMI 2650 nasal cell model to a 3D printed apparatus for the testing of drug deposition and permeation of nasal products. *Eur. J. Pharm. Biopharm.* 107, 223–233. <https://doi.org/10.1016/j.ejpb.2016.07.010>.
- Rajbanshi, A., et al., 2022. Polymer architecture dictates thermoreversible gelation in engineered emulsions stabilised with branched copolymer surfactants. *Polym. Chem.* 13 (40), 5730–5744. <https://doi.org/10.1039/d2py00876a>.
- Rajbanshi, A., et al., 2023a. Branched Copolymer Surfactants as Versatile Templates for Responsive Emulsifiers with Bespoke Temperature-Triggered Emulsion-Breaking or Gelation. *Adv. Mater. Interfaces*, 2300755. <https://doi.org/10.1002/admi.202300755>.
- Rajbanshi, A., et al., 2023b. Combining branched copolymers with additives generates stable thermoresponsive emulsions with in situ gelation upon exposure to body temperature. *Int. J. Pharm.* 637, 122892. <https://doi.org/10.1016/j.ijpharm.2023.122892>.
- Rajbanshi, A., et al., 2024. Stimuli-Responsive Polymers for Engineered Emulsions. *Macromol. Rapid Commun.*, 2300723. <https://doi.org/10.1002/marc.202300723>.

- Rama Prasad, Y.V., Krishnaiah, Y.S.R., Satyanarayana, S., 1996. Intranasal drug delivery systems: An overview. *Indian J. Pharm. Sci.* 58 (1), 1–8. <https://doi.org/10.12691/ajps-3-5-2>.
- Rassu, G., et al., 2017. Nose-to-brain delivery of BACE1 siRNA loaded in solid lipid nanoparticles for Alzheimer's therapy. *Colloids Surf. B Biointerfaces* 152, 296–301. <https://doi.org/10.1016/j.colsurfb.2017.01.031>.
- Recipharm, no date. *Nasal spray device manufacturer, Unidose nasal spray*. <https://www.recipharm.com/drug-delivery-devices/nasal-sprays> (Accessed: 9 August 2023).
- Saindane, N.S., Pagar, K.P., Vavia, P.R., 2013. Nanosuspension based in situ gelling nasal spray of carvedilol: Development, in vitro and in vivo characterization. *AAPS PharmSciTech* 14 (1), 189–199. <https://doi.org/10.1208/s12249-012-9896-y>.
- Sandoz Limited, 2022. *Budesonide 64 micrograms/actuation, Aqueous Nasal Spray*. <https://www.medicines.org.uk/emc/product/445/smpc/print> (Accessed: 16 August 2023).
- Sandri, G., et al., 2012. The role of chitosan as a mucoadhesive agent in mucosal drug delivery. *J. Drug Delivery Sci. Technol.* 22 (4), 275–284. [https://doi.org/10.1016/s1773-2247\(12\)50046-8](https://doi.org/10.1016/s1773-2247(12)50046-8).
- Sarheed, O., Dibi, M., Ramesh, K.V.R.N.S., 2020. Studies on the effect of oil and surfactant on the formation of alginate-based O/W lidocaine nanocarriers using nanoemulsion template. *Pharmaceutics* 12 (12), 1–21. <https://doi.org/10.3390/pharmaceutics12121223>.
- Smart, J.D., 2005. The basics and underlying mechanisms of mucoadhesion. *Adv. Drug Deliv. Rev.* 57 (11), 1556–1568. <https://doi.org/10.1016/j.addr.2005.07.001>.
- Sogias, I.A., Williams, A.C., Khutoryanskiy, V.V., 2008. Why is chitosan mucoadhesive? *Biomacromolecules* 9 (7), 1837–1842. <https://doi.org/10.1021/bm800276d>.
- Trows, S., et al., 2014. Analytical challenges and regulatory requirements for nasal drug products in Europe and the U.S. *Pharmaceutics* 6 (2), 195–219. <https://doi.org/10.3390/pharmaceutics6020195>.
- Vanukuru, S., et al., 2024. Functionalisation of chitosan with methacryloyl and crotonoyl groups as a strategy to enhance its mucoadhesive properties. *Eur. J. Pharm. Biopharm.* 205, 114575. <https://doi.org/10.1016/j.ejpb.2024.114575>.
- VCCLAB, no date. *Virtual Computational Chemistry Laboratory*. <https://vcclab.org/lab/a/logs/> (Accessed: 9 August 2023).
- Vigani, B., et al., 2020. Recent advances in the development of in situ gelling drug delivery systems for non-parenteral administration routes. *Pharmaceutics* 12 (9), 1–29. <https://doi.org/10.3390/pharmaceutics12090859>.
- Wingrove, J., et al., 2019. Characterisation of nasal devices for delivery of insulin to the brain and evaluation in humans using functional magnetic resonance imaging. *J. Control. Release* 302, 140–147. <https://doi.org/10.1016/j.jconrel.2019.03.032>.